The Open Dentistry Journal
DOI: 10.2174/0111992603300611144, 2026, 20, e187421061199
ISSN: 1874-2106
1

RESEARCH ARTICLE **OPEN ACCESS**

CBCT-based Morphological Assessment of the Mandibular Premolar and Molar Regions for Immediate Implant Placement in Vietnamese Adults: A Preliminary Study

Nguyen Ngoc Phuc[1], Nguyen Minh Trung[2], Tran Thị Uyen Phuong[2], Chu Hien Thao[2], Dinh Huu Loc[2], Hoang Trong Chien[2] and Tran Hung Lam[3,*]

[1]*Department of Periodontology and Implantology, Faculty of Dentistry, Van Lang University, Ho Chi Minh City, Vietnam*
[2]*Faculty of Dentistry, Van Lang University, Ho Chi Minh City, Vietnam*
[3]*Department of Prosthodontics, Faculty of Dentistry, Van Lang University, Ho Chi Minh City, Vietnam*

Abstract:

Introduction / Background: Immediate implant placement in the posterior mandible requires precise assessment of alveolar bone morphology due to proximity to the Inferior Alveolar Nerve (IAN) and variable cortical anatomy. Population-specific morphometric data for Vietnamese adults remain limited.

Materials and Methods: This preliminary cross-sectional study retrospectively analyzed 42 Cone-Beam Computed Tomography (CBCT) scans of Vietnamese adults. Virtual Straumann® implants were simulated at mandibular premolar and molar sites. Measurements included implant length, distance to the IAN, buccolingual and proximal bone thickness, mandibular cross-sectional morphology (Chan classification), and interradicular relationship (Chen classification). Statistical analyses were performed using t-tests, Mann–Whitney U tests, and one-way ANOVA.

Results: Mean implant lengths ranged from 15.07 ± 1.28 to 15.93 ± 1.68 mm. The second molar demonstrated the shortest mean distance to the IAN (0.06 ± 2.13 mm), with simulated canal encroachment in 23.8% of cases. Buccal bone thickness increased apically in molars, while lingual bone showed site-specific thinning. U-type mandibular morphology predominated (40–48%), and the septal interradicular relationship was most frequent (56–64%).

Discussion: Compared with Western populations, Vietnamese adults exhibited reduced IAN clearance and a higher prevalence of U-type mandibular morphology, resembling patterns reported in East Asian cohorts. These anatomical features explain the increased risk of neurovascular injury and cortical perforation during immediate implant placement in posterior mandibular sites.

Conclusion: Vietnamese adults exhibit population-specific mandibular morphology characterized by limited IAN clearance and frequent U-shaped cross-sections in the posterior regions. CBCT-guided virtual planning is essential for optimizing implant positioning and ensuring surgical safety.

Keywords: *C*BCT, Mandible, Immediate implant placement, Inferior alveolar nerve, Morphometry, Vietnamese population.

*Address correspondence to this author at the Department of Prosthodontics, Faculty of Dentistry, Van Lang University, Ho Chi Minh City, 70000, Vietnam; E-mail: lam.th@vlu.edu.vn

Cite as: Phuc N, Trung N, Phuong T, Thao C, Loc D, Chien H, Lam T. CBCT-based Morphological Assessment of the Mandibular Premolar and Molar Regions for Immediate Implant Placement in Vietnamese Adults: A Preliminary Study. Open Dent J, 2026; 20: e187421061199. http://dx.doi.org/10.2174/0111992603300611144

Received: October 21, 2025
Revised: December 24, 2025
Accepted: February 06, 2026
Published: May 22, 2026

1. INTRODUCTION

Dental implant therapy has become the gold standard for replacing missing teeth, providing long-term functional and esthetic rehabilitation with high survival rates documented in multiple meta-analyses and systematic reviews. Among the different protocols for implant placement, immediate (within 48 hours after extraction), early (4–8 weeks), and delayed (beyond 8 weeks), the immediate implant approach has gained popularity because it minimizes treatment time, preserves alveolar bone contour, and reduces the number of surgical procedures. However, this technique demands meticulous case selection and precise pre-surgical assessment, as insufficient bone support or misjudged anatomical structures can lead to implant failure or neurovascular complications [1-3].

The posterior mandible poses particular challenges for immediate implant placement. This region is characterized by dense cortical bone, variable ridge morphology, and close proximity to vital structures, including the Inferior Alveolar Nerve (IAN) and the lingual concavity. Inadequate evaluation of these anatomical features increases the risk of cortical plate perforation, nerve injury, and compromised primary stability. Traditional two-dimensional radiographs, including panoramic and periapical images, are limited in depicting the true three-dimensional bone anatomy, especially the buccolingual contour and canal trajectory [4, 5].

In recent years, Cone-Beam Computed Tomography (CBCT), combined with virtual implant planning software, has become an indispensable diagnostic tool. CBCT provides a precise 3D assessment of alveolar bone dimensions, cortical thickness, and proximity to the IAN canal, while virtual planning allows simulation of implant position, angulation, and depth before surgery. Numerous studies have reported population-specific variations in mandibular morphology using CBCT-based analyses, emphasizing that bone anatomy can differ significantly across ethnic groups. For instance, Chan *et al*. classified mandibular cross-sectional morphology into C-, P-, and U-shaped types, and described interradicular relationships relevant to implant positioning [6-8].

However, corresponding morphometric data for Vietnamese individuals remain limited. This study aimed to analyze mandibular morphology at premolar and molar sites using CBCT and virtual implant simulation to provide population-specific data for safer immediate implant placement in Vietnamese patients.

2. MATERIALS AND METHODS

2.1. Study Design

This study adopted a descriptive cross-sectional design based on retrospective analysis of CBCT data. All CBCT scans were obtained from patients who visited the Faculty of Dentistry at Van Lang University in Ho Chi Minh City, Vietnam, between September 2024 and September 2025. Ethical approval for the study protocol was granted by the Van Lang University Institutional Review Board (No. 17/2025/HDDD-IRB-VN-01.078). All procedures complied with the Declaration of Helsinki, and patient data were anonymized prior to analysis.

The sample size of 42 CBCT scans was selected based on feasibility and consistency with previous CBCT-based morphometric studies evaluating mandibular implant sites, which commonly included 30–50 scans for exploratory anatomical analyses [5, 6]. Given the descriptive and preliminary nature of the present study, this sample was considered adequate to identify site-specific anatomical trends and generate population-specific reference data rather than to test causal hypotheses or clinical outcomes.

2.2. Selection Criteria

A total of 42 CBCT scans were included based on predefined inclusion and exclusion criteria.

Inclusion criteria were:

- Adult patients (≥18 years) with complete dentition from mandibular teeth #31 to #37.
- Availability of high-quality CBCT scans that clearly visualized the alveolar bone and the inferior alveolar canal.
- Absence of periapical pathology or significant alveolar bone resorption in the examined region.

Exclusion criteria included:

- CBCT images with motion artifacts, poor resolution, or incomplete coverage of the mandibular posterior region.
- Evidence of periodontal or periapical lesions, cysts, or previous implant or surgical intervention in the examined area.
- Anatomical deformities or systemic conditions affecting bone morphology.

2.3. CBCT Imaging Protocol

All CBCT scans were obtained using a Planmeca ProMax® 3D Mid system (Planmeca, Helsinki, Finland) with standardized acquisition parameters:

- Tube voltage: 90 kVp
- Tube current: 10 mA
- Field of view (FOV): 16 × 9 cm
- Voxel size: 0.2 mm
- Exposure time: 18 seconds

Images were exported in DICOM format and processed using Blue Sky Plan 4.0 software (Blue Sky Bio, USA) for three-dimensional evaluation and virtual implant simulation [9, 10].

2.4. Virtual Implant Simulation

For each CBCT scan, virtual implants were positioned at four sites on the left mandibular quadrant: first premolar (#34), second premolar (#35), first molar (#36), and second molar (#37).

Implant positioning followed the protocol proposed by Chen *et al*. (2021) for virtual immediate implant placement:

- The implant axis was aligned along the long axis of the corresponding tooth.
- The implant platform center was positioned 1 mm apical to the buccal alveolar crest.
- The implant apex extended approximately 4 mm beyond the root apex on the sagittal plane.
- Two implant types (Straumann®, Basel, Switzerland) were simulated:
- Premolar sites: 4.1 mm platform diameter, 2.7 mm apical diameter.
- Molar sites: 4.8 mm platform diameter, 3.2 mm apical diameter.

The implant length was adjusted according to the available vertical bone height to avoid IAN canal invasion.

2.5. Morphological Measurements

Following virtual implant placement, measurements were obtained on both sagittal and cross-sectional planes. The following parameters were recorded:

- Implant length (mm): vertical distance from the platform to the apex.
- IAN: shortest distance from the implant apex to the superior border of the IAN canal. Negative values indicated simulated nerve encroachment.
- Buccal and lingual bone thickness (mm): horizontal distances from implant surface to respective cortical plates at 1 mm, 3 mm, 5 mm, 7 mm, and 9 mm apical to the buccal crest.
- Mesial and distal bone thickness (mm): distances between the implant surface and proximal alveolar walls on the same cross-sectional levels.
- Mandibular cross-sectional shape: classified as C-, P-, or U-type according to Chan *et al*. [11] based on sagittal morphology.
- Interradicular relationship: Categorized as Mesial (M), Septal (S), or Mesial–Septal (M–S) types according to Chen *et al*. [6] based on the coronal view.

2.6. Reliability Assessment

All measurements were performed by a single examiner who had undergone standardized training in CBCT interpretation and virtual implant planning. To assess intra-examiner reliability, 10 CBCT scans were randomly selected and measured twice at a one-month interval under identical conditions. The intraclass correlation coefficient (ICC) was computed using a two-way mixed-effects model. An ICC value > 0.80 was considered indicative of excellent reliability.

2.7. Data Statistics

All data were entered into Microsoft Excel and analyzed using IBM SPSS version 25.0 (IBM Corp., Armonk, NY, USA). Data normality was assessed with the Shapiro–Wilk test. Descriptive statistics, including mean, standard deviation, and range, were calculated for all quantitative variables. For comparisons between the premolar and molar groups, the independent-samples t-test was employed, or the Mann–Whitney U test when data were not normally distributed. Differences among measurements at various slice levels (1–9 mm) were analyzed using a one-way ANOVA followed by a Bonferroni post hoc test. A *p*-value of less than 0.05 was considered statistically significant.

3. RESULTS

3.1. Participant Characteristics

A total of 42 CBCT scans from Vietnamese adults (mean age: 34.2 ± 8.7 years; 21 males and 21 females) were analyzed. All scans met the predefined inclusion and exclusion criteria. Virtual Straumann® implants were successfully simulated at four mandibular sites per scan (first and second premolars, first and second molars), resulting in 168 implant positions in total. Intra-examiner reliability was excellent for all parameters (ICC = 0.92–0.98; $p < 0.001$).

3.2. Implant Dimensions and Proximity to Inferior Alveolar Nerve

Simulated implant lengths ranged from 12 mm to 19 mm, with mean values between 15.07 ± 1.28 mm and 15.93 ± 1.68 mm. The shortest mean distance from the implant apex to the IAN canal was recorded at the second molar (0.06 ± 2.13 mm), followed by the second premolar (1.48 ± 2.38 mm), first molar (1.73 ± 2.24 mm), and first premolar (4.31 ± 2.35 mm). Negative values indicating simulated canal encroachment were found in 23.8% of second molar and 19.0% of second premolar sites ($p < 0.05$ compared with premolars) (Table **1**). Representative sagittal CBCT images demonstrate the critically reduced distance between the virtual implant apex and the IAN canal at posterior mandibular sites, particularly at the second molar region (Fig. **1**).

Table 1. Implant dimensions and distance to the inferior alveolar nerve canal (n = 42).

Site	Implant Length (mm)	Distance to IAN (mm)	Encroachment (%)
1st Premolar	15.12 ± 1.49	4.31 ± 2.35	0
2nd Premolar	15.93 ± 1.68	1.48 ± 2.38	19.0
1st Molar	15.26 ± 1.45	1.73 ± 2.24	16.7
2nd Molar	15.07 ± 1.28	0.06 ± 2.13	23.8

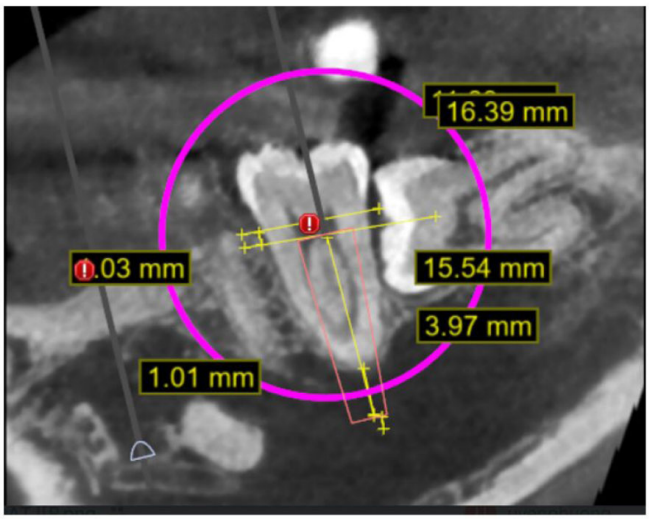

Fig. (1). Site-specific relationship between virtual implant placement and the inferior alveolar nerve in the posterior mandible. Representative sagittal CBCT image showing virtual immediate implant placement at the mandibular left second molar (#37). The implant axis was aligned with the long axis of the tooth, and the platform was positioned 1 mm apical to the buccal crest. The shortest distance between the implant apex and the superior border of the inferior alveolar nerve (IAN) canal is illustrated. This figure demonstrates the critically reduced safety margin and potential nerve encroachment commonly observed at posterior mandibular sites, particularly the second molar region.

3.3. Buccolingual and Proximal Bone Dimensions

At the premolar regions, buccal bone thickness decreased apically, from 2.58 mm at 1 mm below the crest to 1.63 mm at 9 mm, while the lingual plate thickened from 3.16 mm to 5.32 mm. The second premolar showed a more uniform buccal dimension (~2.4 mm) and a greater lingual expansion (up to 5.35 mm). Narrow mesial and distal walls (< 1 mm) were common, with occasional cortical perforations.

In the molar regions, buccal bone thickness increased progressively with depth—from 3.12 mm to 4.41 mm in the first molar and up to 8.04 ± 1.80 mm in the second molar—while lingual bone slightly thinned beyond the mid-apical level. ANOVA confirmed significant differences in buccal thickness at 7–9 mm levels between premolars and molars ($p < 0.01$) and in lingual thickness between the two molars ($p < 0.05$) (Table **1**).

3.4. Mandibular Morphology and Interradicular Relationship

Among molar sites, the U-type mandibular shape (Chan *et al.*) was the most prevalent, observed in 47.6% of first molars and 40.5% of second molars. The Septal (S) type interradicular relationship (Chen *et al.*) predominated at both sites, accounting for 64.3% and 56.1%, respectively.

The coexistence of U-type cross-sections and S-type relationships suggests a pattern of concave lingual morphology with strong septal bone anchorage, offering both surgical risk and mechanical stability during immediate implant placement. This combined analysis demonstrates that the mandibular molar region in Vietnamese adults predominantly exhibits a U-type cross-sectional profile with septal bone engagement, providing useful guidance for implant planning and risk assessment (Table **2**). Sagittal CBCT images illustrating the three mandibular cross-sectional morphology types according to the Chan classification are presented in Fig. (**2**), with the U-type morphology predominating in the molar regions. The interradicular relationship patterns of virtual implants, classified as mesial (M), septal (S), and mesial–septal (M–S), are illustrated in Fig. (**3**), with the septal (S) type being the most prevalent in both mandibular molars.

4. DISCUSSION

The CBCT-based virtual implant study provided population-specific morphometric data of the mandibular premolar and molar regions in Vietnamese adults and highlights distinct site-specific anatomical trends relevant to immediate implant placement. While the imaging technique itself is well established, the present findings contribute novel insights by characterizing mandibular morphology in a Southeast Asian population that remains underrepresented in the existing literature [12, 13].

A major finding of this study is the critically reduced safety margin between the implant apex and the IAN, particularly at the second premolar and second molar sites. The mean IAN distance at the second molar was only 0.06 ± 2.13 mm, with frequent negative values indicating simulated canal encroachment. These observations, illustrated in Fig. (**1**), confirm that the posterior mandible, especially the second molar region, constitutes a high-risk zone for neurosensory complications [14, 15]. Previous studies have generally reported greater IAN clearance at comparable sites. Chrcanovic *et al.* [16] reported mean distances exceeding 3–4 mm in Brazilian cohorts, suggesting a wider anatomical safety margin. The narrower clearance observed in the present Vietnamese sample may reflect ethnic differences in mandibular height, canal trajectory, or alveolar crest morphology, underscoring the importance of population-specific reference data [17-19].

Table 2. Mandibular morphology and interradicular relationship at molar regions.

Site	C-type (%)	P-type (%)	U-type (%)	Dominant Shape	Mesial (%)	Septal (%)	Mesial-Septal (%)	Dominant Relationship
1st Molar	21.4	31.0	47.6	U-type	4.8	64.3	31.0	S-type
2nd Molar	35.7	23.8	40.5	U-type	4.9	56.1	39.0	S-type

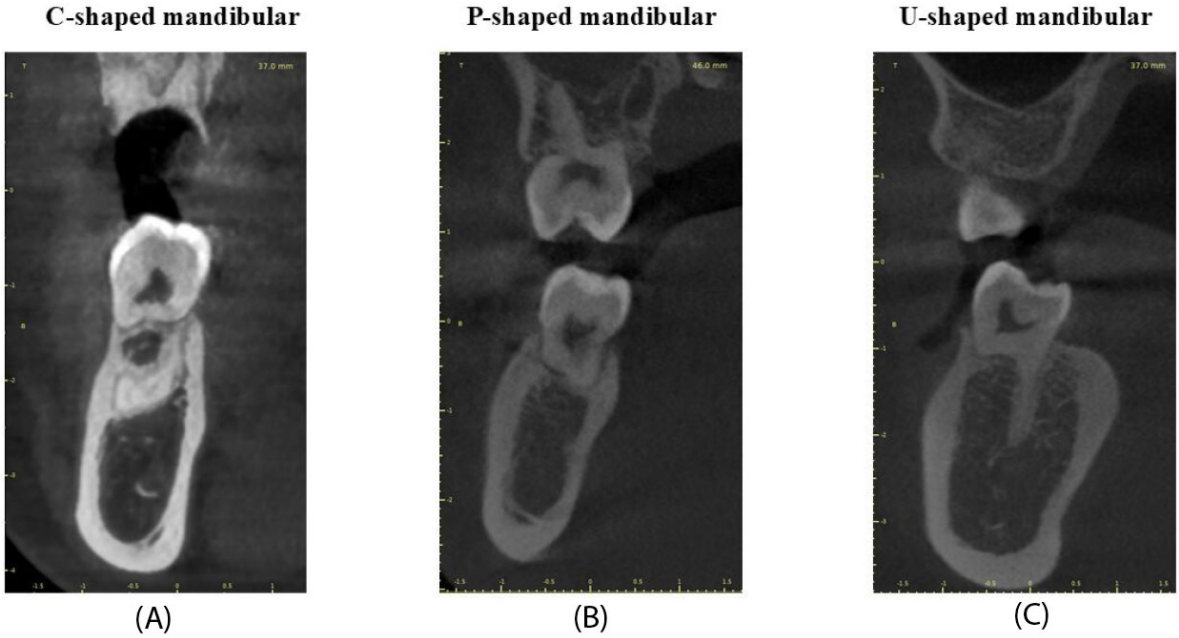

Fig. (2). Mandibular cross-sectional morphology according to the Chan classification. Sagittal CBCT views illustrating the three mandibular cross-sectional morphology types as classified by Chan *et al*.: (**A**) C-type, characterized by convergence of buccal and lingual cortical plates at the crestal level; (**B**) P-type, where buccal and lingual plates run approximately parallel; and (**C**) U-type, defined by a distinct lingual concavity. In this study cohort, the U-type morphology predominated in the molar regions, explaining the increased risk of lingual plate perforation during immediate implant placement in the Vietnamese mandible.

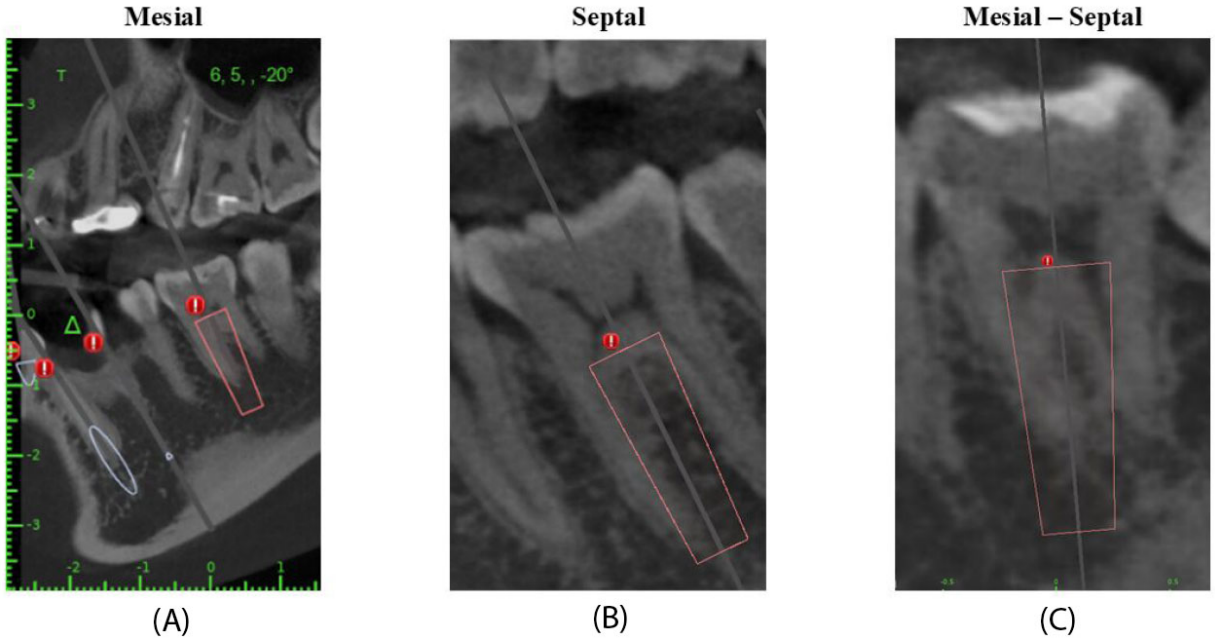

Fig. (3). Interradicular relationship patterns of virtual implants in mandibular molar regions. Coronal CBCT views illustrating interradicular relationship patterns based on the classification proposed by Chen *et al*.: (**A**) Mesial (M) type, where the implant axis passes only through the mesial root; (**B**) Septal (S) type, where the implant axis engages the interradicular septal bone; and (**C**) Mesial–Septal (M–S) type, involving both mesial root and septal bone. The septal (S) relationship was the most prevalent pattern in both mandibular molars, suggesting favorable septal bone engagement and potential for improved primary stability during immediate implant placement.

Distinct buccolingual bone thickness trends were also identified across tooth groups. In the premolar region, buccal bone thickness decreased progressively toward the apex, particularly at the first premolar, whereas lingual thickness increased apically. In contrast, molar sites demonstrated marked buccal bone expansion with increasing depth, while lingual bone thickness showed greater variability and, in some cases, apical thinning, most notably at the second molar. These site-specific patterns explain the occurrence of negative lingual values and potential cortical perforation risks observed in the deeper slices [4]. Such trends are consistent with East Asian CBCT studies, including those by Huang *et al*. [5] and Chen *et al*. [6]; however, they differ from several Western reports in which lingual concavity appears less pronounced. The anatomical implications of these differences are clinically significant, as excessive lingual undercuts may predispose to perforation during immediate implant placement if implant angulation and depth are not carefully controlled [20, 21].

Mandibular cross-sectional morphology further clarifies these findings. In the present cohort, the U-type mandible predominated in the molar region, accounting for approximately 40–48% of cases, as shown in Fig. (**2**). This distribution contrasts with studies conducted in Western populations, where P-type morphology has often been reported as the most prevalent. Conversely, our results closely resemble those reported in Taiwanese and mainland Chinese populations, in which U-type morphology is also common. The U-type configuration, characterized by a pronounced lingual concavity, provides a plausible anatomical explanation for both the reduced lingual bone thickness and the increased perforation risk observed in this study. These findings suggest that ethnic and regional anatomical variation should be considered an essential factor in implant risk assessment rather than assuming universal mandibular morphology [5].

The interradicular relationship analysis revealed that the Septal (S) pattern was the most prevalent at both molar sites, followed by the mesial–septal (M–S) and mesial (M) types. As illustrated in Fig. (**3**), septal engagement offers favorable conditions for primary implant stability, particularly in immediate placement scenarios. This observation supports the feasibility of immediate implant placement in mandibular molars of Vietnamese patients when adequate septal bone is present, despite the elevated neurovascular and cortical risks [22]. While Chen *et al*. reported similar findings for first molars in Chinese populations, differences were noted at second molar sites, where mesial engagement was more common in their cohort. These discrepancies may again reflect population-specific anatomical variations or differences in sample size and implant simulation protocols.

The present findings emphasize that the mandibular posterior region in Vietnamese adults exhibits a unique combination of anatomical advantages and risks: abundant buccal bone and frequent septal engagement favor primary stability, whereas reduced IAN clearance and prevalent U-type morphology increase the risk of neurovascular injury and cortical perforation. The integration of CBCT-based virtual implant planning, as demonstrated in this study, enables clinicians to visualize these site-specific trends preoperatively and to individualize implant length, diameter, and angulation accordingly [23, 24].

5. STUDY LIMITATIONS

This study was limited by its modest sample size and single-center design, which may not fully capture population variability. Moreover, virtual simulations cannot reproduce clinical factors such as socket remodeling or intraoperative bone compression. Larger, multicenter CBCT studies and clinical trials are recommended to validate these findings and develop a comprehensive Vietnamese morphometric database for implant dentistry.

CONCLUSION

This study established essential CBCT-based reference data for immediate implant placement. The second premolar and molar regions were found to be closest to the inferior alveolar nerve, underscoring the need for cautious depth control and a minimum safety clearance of 2 mm. The predominance of U-type mandibular morphology and Septal interradicular relationships suggests both higher perforation risk and favorable primary stability when properly planned. These findings highlight the importance of individualized, CBCT-guided virtual planning to ensure safe and predictable outcomes. Larger multicenter studies are recommended to validate these anatomical patterns and support the development of a national morphometric database for implant dentistry.

AUTHORS' CONTRIBUTIONS

The authors confirm their contributions to the paper as follows: N.N.P. and T.H.L. contributed to study conception and design; N.M.T., T.T.U.P., C.H.T., D.H.L., and H.T.C. carried out data collection; N.N.P., T.H.L., and N.M.T. performed the analysis and interpretation of the results; and N.M.T. and T.T.U.P. prepared the draft manuscript. All authors reviewed the results and approved the final version of the manuscript.

LIST OF ABBREVIATIONS

IAN	=	Inferior Alveolar Nerve
CBCT	=	Cone-Beam Computed Tomography
ICC	=	Intraclass Correlation Coefficient

ETHICS APPROVAL AND CONSENT TO PARTICIPATE

Ethical approval for the study protocol was granted by the Van Lang University Institutional Review Board (No. 17/2025/HDDD-IRB-VN-01.078).

HUMAN AND ANIMAL RIGHTS

All human research procedures followed were in accordance with the ethical standards of the committee

responsible for human experimentation (institutional and national), and with the Helsinki Declaration of 1975, as revised in 2013.

CONSENT FOR PUBLICATION

Not applicable.

STANDARDS OF REPORTING

STROBE guidelines were followed.

AVAILABILITY OF DATA AND MATERIALS

The data and supportive information are available within the article.

FUNDING

None.

CONFLICT OF INTEREST

The authors declare no conflict of interest, financial or otherwise.

ACKNOWLEDGEMENTS

Declared none.

REFERENCES

[1] Garcia-Sanchez R, Dopico J, Kalemaj Z, Buti J, Pardo Zamora G, Mardas N. Comparison of clinical outcomes of immediate *versus* delayed placement of dental implants: A systematic review and meta-analysis. Clin Oral Implants Res 2022; 33(3): 231-77. http://dx.doi.org/10.1111/clr.13892 PMID: 35044012

[2] Ragucci GM, Elnayef B, Criado-Cámara E, Del Amo FSL, Hernández-Alfaro F. Immediate implant placement in molar extraction sockets: A systematic review and meta-analysis. Int J Implant Dent 2020; 6(1): 40. http://dx.doi.org/10.1186/s40729-020-00235-5 PMID: 32770283

[3] Atieh MA, Alsabeeha NHM, Duncan WJ, *et al*. Immediate single implant restorations in mandibular molar extraction sockets: A controlled clinical trial. Clin Oral Implants Res 2013; 24(5): 484-96. http://dx.doi.org/10.1111/j.1600-0501.2011.02415.x PMID: 22276690

[4] Wang TY, Kuo PJ, Fu E, *et al*. Risks of angled implant placement on posterior mandible buccal/lingual plated perforation: A virtual immediate implant placement study using CBCT. J Dent Sci 2019; 14(3): 234-40. http://dx.doi.org/10.1016/j.jds.2019.03.005 PMID: 31528250

[5] Huang RY, Cochran DL, Cheng WC, *et al*. Risk of lingual plate perforation for virtual immediate implant placement in the posterior mandible. J Am Dent Assoc 2015; 146(10): 735-42. http://dx.doi.org/10.1016/j.adaj.2015.04.027 PMID: 26409983

[6] Chen H, Wang W, Gu X. Three-dimensional alveolar bone assessment of mandibular molars for immediate implant placement: A virtual implant placement study. BMC Oral Health 2021; 21(1): 478. http://dx.doi.org/10.1186/s12903-021-01849-w PMID: 34579702

[7] Sun Y, Hu S, Xie Z, Zhou Y. Relevant factors of posterior mandible lingual plate perforation during immediate implant placement: A virtual implant placement study using CBCT. BMC Oral Health 2023; 23(1): 76. http://dx.doi.org/10.1186/s12903-022-02696-z PMID: 36747164

[8] Sivolella S, Meggiorin S, Ferrarese N, *et al*. CT-based dentulous mandibular alveolar ridge measurements as predictors of crown-to-implant ratio for short and extra short dental implants. Sci Rep 2020; 10(1): 16229. http://dx.doi.org/10.1038/s41598-020-73180-3 PMID: 33004827

[9] Kernen F, Kramer J, Wanner L, Wismeijer D, Nelson K, Flügge T. A review of virtual planning software for guided implant surgery - data import and visualization, drill guide design and manufacturing. BMC Oral Health 2020; 20(1): 251. http://dx.doi.org/10.1186/s12903-020-01208-1 PMID: 32912273

[10] Landfald IC, Łapot M, Olewnik Ł. Imaging-based clinical management of mandibular canal variants: PR–CBCT–selective MRI. Biomedicines 2025; 13(11): 2760. http://dx.doi.org/10.3390/biomedicines13112760 PMID: 41301854

[11] Chan HL, Benavides E, Yeh CY, Fu JH, Rudek IE, Wang HL. Risk assessment of lingual plate perforation in posterior mandibular region: A virtual implant placement study using cone-beam computed tomography. J Periodontol 2011; 82(1): 129-35. http://dx.doi.org/10.1902/jop.2010.100313 PMID: 20653440

[12] Abbas MJ, Al-Khatib AR, Hassan NA, Aljoujou AA, ALhomsi A, ALsalim MW. CBCT dual-center investigation of relationship between the inferior alveolar canal and the lingual mandibular depression of the submandibular salivary glands. Sci Rep 2025; 15(1): 42992. http://dx.doi.org/10.1038/s41598-025-26973-3 PMID: 41330967

[13] Rajkovic Pavlovic Z, Stepovic M, Bubalo M, *et al*. Anatomic variations important for dental implantation in the mandible—A systematic review. Diagnostics 2025; 15(2): 155. http://dx.doi.org/10.3390/diagnostics15020155 PMID: 39857039

[14] Leong DJM, Chan HL, Yeh CY, Takarakis N, Fu JH, Wang HL. Risk of lingual plate perforation during implant placement in the posterior mandible: A human cadaver study. Implant Dent 2011; 20(5): 360-3. http://dx.doi.org/10.1097/ID.0b013e3182263555 PMID: 21811168

[15] Juodzbalys G, Wang HL, Sabalys G. Injury of the inferior alveolar nerve during implant placement: A literature review. J Oral Maxillofac Res 2011; 2(1): e1. http://dx.doi.org/10.5037/jomr.2011.2101 PMID: 24421983

[16] Chrcanovic BR, de Carvalho Machado V, Gjelvold B. Immediate implant placement in the posterior mandible: A cone beam computed tomography study. Quintessence Int 2016; 47(6): 505-14. http://dx.doi.org/10.3290/j.qi.a36008 PMID: 27092357

[17] Shi Q, Huang Y, Huo N, Jiang Y, Zhang T, Wang J. Restoration-oriented anatomical analysis of alveolar bone at mandibular first molars and implications for immediate implant placement surgery: A CBCT study. J Adv Prosthodont 2024; 16(4): 212-20. http://dx.doi.org/10.4047/jap.2024.16.4.212 PMID: 39221416

[18] Geng N, Ren J, Zhang C, Zhou T, Feng C, Chen S. Immediate implant placement in the posterior mandibular region was assisted by dynamic real-time navigation: A retrospective study. BMC Oral Health 2024; 24(1): 208. http://dx.doi.org/10.1186/s12903-024-03947-x PMID: 38336661

[19] Dung SZ, Wang J, Weng TH, Tu YK. Long-term outcomes and risk assessment of immediate implants at molar extraction sites in a Taiwan population. Sci Rep 2025; 15(1): 23333. http://dx.doi.org/10.1038/s41598-025-06048-z PMID: 40603356

[20] Alqutaibi AY, Alghauli MA, Aboalrejal A, *et al*. Quantitative and qualitative 3D analysis of mandibular lingual concavities: Implications for dental implant planning in the posterior mandible. Clin Exp Dent Res 2024; 10(1): e858. http://dx.doi.org/10.1002/cre2.858 PMID: 38345362

[21] Mukherjee S, Bajoria AA, N C S, Bhuvaneshwari S, Mishra S, Singh D. Proposed classification system for submandibular gland fossa anatomy and its radiomorphometric assessment using cone-beam computed tomography: A retrospective study. Cureus 2025; 17(1): e77301. http://dx.doi.org/10.7759/cureus.77301 PMID: 39944454

[22] Witoonkitvanich P, Amornsettachai P, Panyayong W, Rokaya D, Vongsirichat N, Suphangul S. Comparison of the stability of immediate dental implant placement in fresh molar extraction sockets in the maxilla and mandible: A controlled, prospective, non-randomized clinical trial. Int J Oral Maxillofac Surg 2025; 54(4): 365-73. http://dx.doi.org/10.1016/j.ijom.2024.12.011 PMID: 39794221

[23] Kanewoff E, Alhallak R, de Carvalho Machado V, Chrcanovic BR. Immediate implant placement in the anterior mandible: A cone beam computed tomography study. BMC Oral Health 2024; 24(1): 393.
http://dx.doi.org/10.1186/s12903-024-04111-1 PMID: 38539122

[24] Hamzani Y, Yassien E, Moskovich L, Becker T, Chaushu G, Haj Yahya B. Potential circumferential bone engagement following tooth extraction in the posterior mandible: Computed tomography assessment. Medicina 2021; 57(9): 874.
http://dx.doi.org/10.3390/medicina57090874 PMID: 34577797